

Natural and Semisynthetic Chalcones as Dual FLT3 and Microtubule Polymerization Inhibitors

Haleema Sadia Malik, Aishah Bilal, Rahim Ullah, Maheen Iqbal, Sardraz Khan, Ishtiaq Ahmed, Karsten Krohn, Rahman Shah Zaib Saleem, Hidayat Hussain,* and Amir Faisal*



Cite This: <https://dx.doi.org/10.1021/acs.jnatprod.0c00699>



Read Online

ACCESS |



Metrics & More

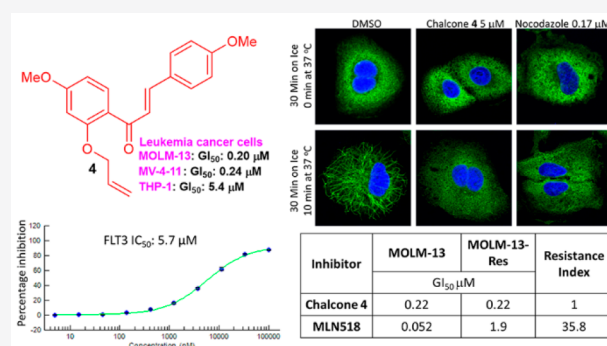


Article Recommendations



Supporting Information

ABSTRACT: Activating mutations in FLT3 receptor tyrosine kinase are found in a third of acute myeloid leukemia (AML) patients and are associated with disease relapse and a poor prognosis. The majority of these mutations are internal tandem duplications (ITDs) in the juxtamembrane domain of FLT3, which have been validated as a therapeutic target. The clinical success of selective inhibitors targeting oncogenic FLT3, however, has been limited due to the acquisition of drug resistance. Herein the identification of a dual FLT3/microtubule polymerization inhibitor, chalcone 4 (2'-allyloxy-4,4'-dimethoxychalcone), is reported through screening of 15 related chalcones for differential antiproliferative activity in leukemia cell lines dependent on FLT3-ITD (MV-4-11) or BCR-ABL (K562) oncogenes and by subsequent screening for mitotic inducers in the HCT116 cell line. Three natural chalcones (1–3) were found to be differentially more potent toward the MV-4-11 (FLT3-ITD) cell line compared to the K562 (BCR-ABL) cell line. Notably, the new semisynthetic chalcone 4, which is a 2'-O-allyl analogue of the natural chalcone 3, was found to be more potent toward the FLT3-ITD+ cell line and inhibited FLT3 signaling in FLT3-dependent cells. An in vitro kinase assay confirmed that chalcone 4 directly inhibited FLT3. Moreover, chalcone 4 induced mitotic arrest in these cells and inhibited tubulin polymerization in both cellular and biochemical assays. Treatment of MV-4-11 cells with this inhibitor for 24 and 48 h resulted in apoptotic cell death. Finally, chalcone 4 was able to overcome TKD mutation-mediated acquired resistance to FLT3 inhibitors in a MOLM-13 cell line expressing FLT3-ITD with the D835Y mutation. Chalcone 4 is, therefore, a promising lead for the discovery of dual-target FLT3 inhibitors.



Three natural chalcones (1–3) were found to be differentially more potent toward the MV-4-11 (FLT3-ITD) cell line compared to the K562 (BCR-ABL) cell line. Notably, the new semisynthetic chalcone 4, which is a 2'-O-allyl analogue of the natural chalcone 3, was found to be more potent toward the FLT3-ITD+ cell line and inhibited FLT3 signaling in FLT3-dependent cells. An in vitro kinase assay confirmed that chalcone 4 directly inhibited FLT3. Moreover, chalcone 4 induced mitotic arrest in these cells and inhibited tubulin polymerization in both cellular and biochemical assays. Treatment of MV-4-11 cells with this inhibitor for 24 and 48 h resulted in apoptotic cell death. Finally, chalcone 4 was able to overcome TKD mutation-mediated acquired resistance to FLT3 inhibitors in a MOLM-13 cell line expressing FLT3-ITD with the D835Y mutation. Chalcone 4 is, therefore, a promising lead for the discovery of dual-target FLT3 inhibitors.

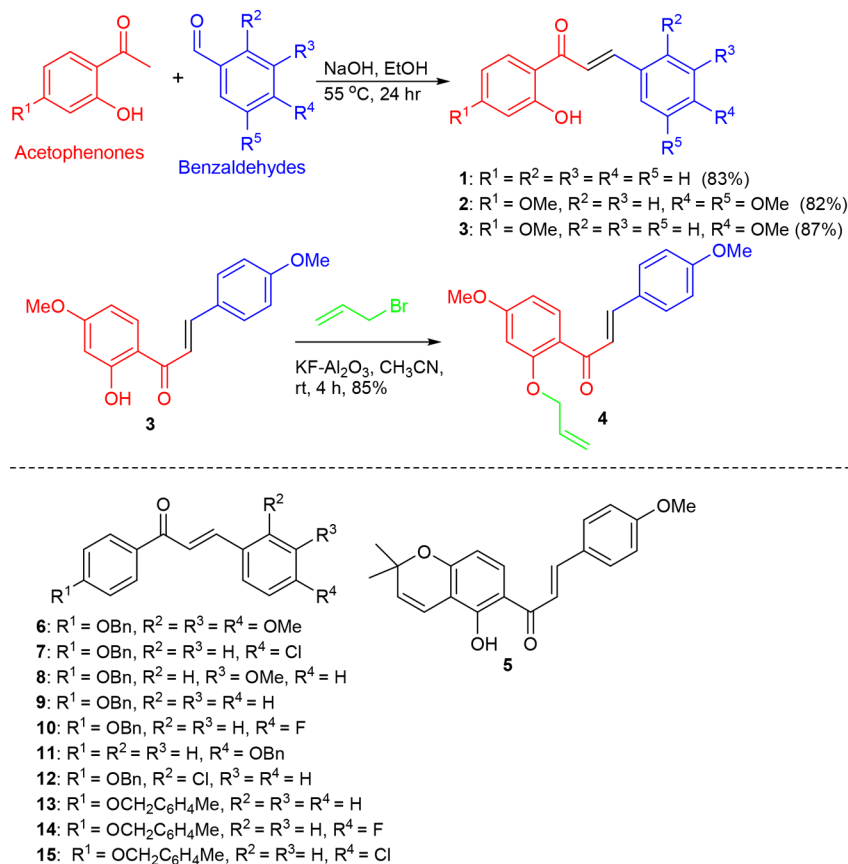
Acute myeloid leukemia (AML) results from interrupted differentiation and maturation of hematopoietic progenitor cells, leading to uncontrolled proliferation and accumulation of myeloid blasts. It is the most frequent form of myeloid leukemia, and more than a quarter of a million adults are diagnosed with this disease each year.^{1,2} Mutations in the nucleophosmin 1 (*NPM1*), FMS-like tyrosine kinase 3 (*FLT3*), and DNA methyltransferase 3A (*DNMT3A*) genes are the most frequent mutations associated with AML. FLT3 belongs to the class III receptor tyrosine kinase (RTK) family, which is characterized by structural features such as extracellular immunoglobulin-like domains, a transmembrane part, a juxtamembrane (JM) domain, and an intracellular tyrosine kinase domain (TKD) split into two.^{3,4} The JM domain plays an inhibitory role and prevents the activation loop from acquiring the active conformation in the absence of the ligand. Binding of the FLT3-ligand (FL) to its receptor causes it to undergo a conformational change leading to its homodimerization and subsequent activation. The internal tandem duplications (ITDs) in the JM domain are the most frequent mutations in FLT3.^{5–7} The ITDs are in-frame insertion of duplicated sequences, which comprise approx-

imately 3–400 base pairs in length and act as gain of function mutations by promoting receptor dimerization in the absence of the ligand, thereby constitutively activating the receptor.⁸ Point mutations in the TKD are less frequent when compared to the ITD mutations and also result in ligand-independent activation of the FLT3 receptor.⁹ Both of these activating mutations are associated with disease relapse and poor prognosis.

Activated FLT3 promotes cell proliferation and survival through multiple downstream signaling pathways, including phosphatidylinositol 3-kinase (PI3K)/AKT, signal transducer and activator of transcription 5 (STAT5), and extracellular signal-regulated kinase (ERK).^{10,11} Many small-molecule FLT3 inhibitors have been developed and evaluated in clinical trials,

Received: June 23, 2020

Scheme 1. Preparation of Chalcones 1–4 and Structures of Chalcones 5–15



including sorafenib,¹² lestaurtinib,¹³ and quizartinib.¹⁴ Two FLT3 inhibitors, midostaurin and gilteritinib, have also been approved for the treatment of FLT3-ITD+ AML patients.^{15,16} The efficacy of many of these inhibitors as a single agent, however, has been limited by transient responses and the development of acquired resistance.^{17,18} Acquisition of secondary mutations in the TKD domain represents the predominant drug resistance mechanism,¹⁹ and mutations at F691 and D835 residues in the TKD domain have been identified in relapsed patients undergoing treatment with FLT3 inhibitors.^{20,21}

Overcoming TKD-mediated drug resistance thus represents a major challenge for the treatment of FLT3-ITD-driven tumors.²² Discovery of drugs that can inhibit FLT3-TKD mutants, administration of drugs in combination and polypharmacology for engagement of targets in addition to FLT3 have been employed to overcome primary and acquired resistance to FLT3 inhibitors.^{23–25} Several dual FLT3 inhibitors have been shown to overcome TKD-mediated drug resistance. Examples of dual FLT3 inhibitors include AMG 925, which inhibits FLT3/CDK4, and tandutinib, which targets FLT3/PDGFR.²³ Similarly, inhibitors that target Aurora kinases in addition to FLT3 can overcome TKD-mediated acquired resistance to FLT3 inhibitors.^{26,27}

Microtubules are dynamic structures that are critical for the completion of mitosis and the division of cells, in addition to their role in cell signaling, vesicular transport, and cytoskeleton dynamics.²⁸ The highly dynamic nature of spindle microtubules has been utilized successfully to target rapidly proliferating cancer cells with drugs that interfere with microtubule dynamics.²⁹ Many small-molecule kinase inhib-

itors have been shown to target microtubule dynamics in addition to their primary targets.³⁰ Tivantinib is a c-Met inhibitor, which, for example, was initially developed to inhibit the proliferation of cells expressing wild-type or mutant forms of c-Met.³¹ It was, however, found to inhibit the proliferation of cells without c-Met expression owing to its ability to bind to microtubules at the colchicine-binding site.^{32,33} Similarly, 3-substituted 7-phenylpyrrolo[3,2-*f*]quinolin-9(6*H*)-one was initially discovered as a microtubule polymerization inhibitor but was later found to inhibit multiple kinases, including FLT3.³⁴

Chalcones are a flavonoid subgroup that are distributed widely in fruits, vegetables, teas, and plants.³⁵ Chalcones have been reported to exhibit numerous biological properties such as anti-inflammatory, antimicrobial, antifungal, antimalarial, antidiabetic, anti-HIV, antiprotozoal, antioxidant, and cytotoxic activities.^{35,36} In addition, several chalcone-based molecules have been authorized for clinical practice.³⁵ Herein are presented the identification and characterization of natural chalcones (1–3) and in particular the semisynthetic chalcone 4 as a dual FLT3/microtubule polymerization inhibitor. Chalcone 4 has been found to be preferentially more active in FLT3-ITD-expressing cells and inhibits FLT3 directly in a biochemical assay. It was also determined that chalcone 4 induces mitotic arrest and inhibits microtubule polymerization *in vitro*. The dual inhibition of FLT3 and microtubules causes apoptotic cell death and is able to overcome D835Y-mediated resistance to FLT3 inhibitors.

Table 1. GI₅₀ Values of Chalcones 1–4 in Three AML Cell Lines

compound no.	GI ₅₀ ± SEM (μM) ^a		
	MOLM-13	MV-4-11	THP-1
1	>10	>10	>10
2	10 ± 1.91 (n = 4)	>10	>100
3	>10	>10	>100
4	0.20 ± 0.096 (n = 3)	0.24 ± 0.015 (n = 3)	5.4 ± 1.615 (n = 4)

^aData represent mean values ± standard error of mean (SEM) for at least two independent biological replicates.

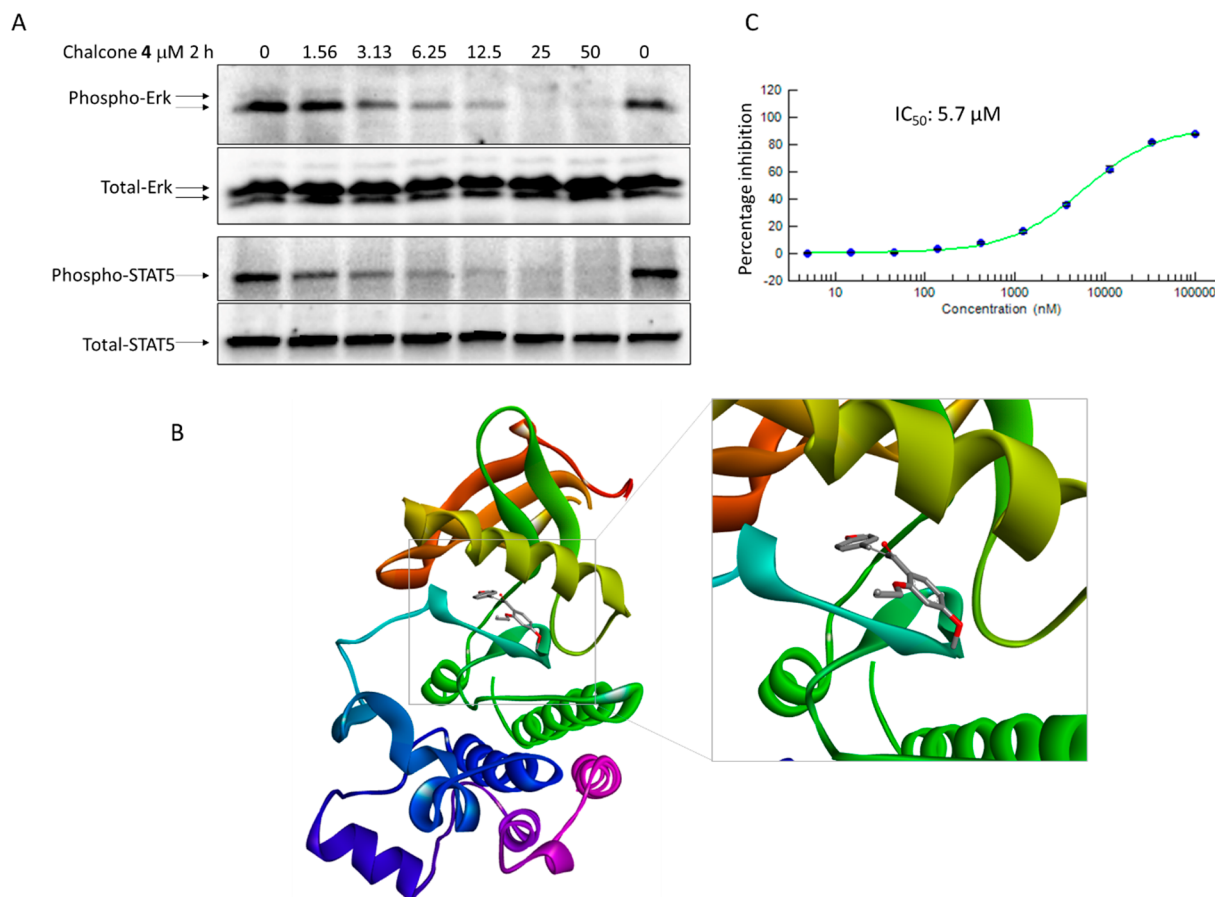


Figure 1. Chalcone 4 is an FLT3 inhibitor. (A) Inhibition of FLT3 downstream signaling by chalcone 4 in MV-4-11 cells. Cells were treated with indicated concentrations of chalcone 4 for 2 h, followed by analysis of Stat5 and Erk phosphorylation through immunoblotting. Levels of total Stat5 and total Erk were used as loading controls. (B) Docking of chalcone 4 with FLT3. (C) Chalcone 4 directly inhibits FLT3. IC₅₀ of chalcone 4 was determined in an FLT3 kinase assay at 10 μM ATP concentration.

RESULTS AND DISCUSSION

Chemistry. The natural chalcones 1–3 and the semi-synthetic new analogue 4 (Scheme 1) were prepared using the Claisen–Schmidt condensation protocol. Furthermore, the new chalcone 4 was prepared by treating natural chalcone 3 with allyl bromide in the presence of KF–Al₂O₃ (Scheme 1). The chalcone 5 (4-methoxyonchocarpin) was isolated from the plant *Dorstenia poinsettifolia*.³⁷ The chemistry of the synthetic chalcones 6–15 was already published by our group.³⁶

Identification of Chalcones as FLT3 Inhibitors. Initially, all the chalcones obtained were screened in leukemia cell lines expressing FLT3-ITD (MV-4-11) or BCR-ABL (K562) at 25 and 50 μM concentrations in three-day MTS proliferation assays. The three natural chalcones, viz., 2'-hydroxychalcone (1),³⁸ 2'-hydroxy-3,4,4'-trimethoxychalcone

(2),³⁹ and 4,4'-dimethoxy-2'-hydroxychalcone (3)^{40,41} (Scheme 1), were found to be differentially more potent toward the MV-4-11 (FLT3-ITD) cell line compared to the K562 (BCR-ABL) cell line at both concentrations [Figure S1, Supporting Information (pink outline)]. It is noteworthy that the new synthesized chalcone 4, which is the 2'-allyloxy analogue of the natural chalcone 3, inhibited the growth of both cell lines by >95% at the two concentrations tested (25 and 50 μM; Figure S1, Supporting Information). However, the natural chalcone 5³⁵ and the semisynthetic chalcones 6–15³⁶ were not effective toward the two cell lines used.

The GI₅₀ values of chalcones 1–4 were next determined in two AML cell lines with oncogenic FLT3-ITD mutations (MV-4-11 and MOLM-13) and one AML cell line with wild-type (WT) FLT3 (THP-1). As shown in Table 1, chalcones 1–3 had GI₅₀ values ≥ 10 μM in all three cell lines with

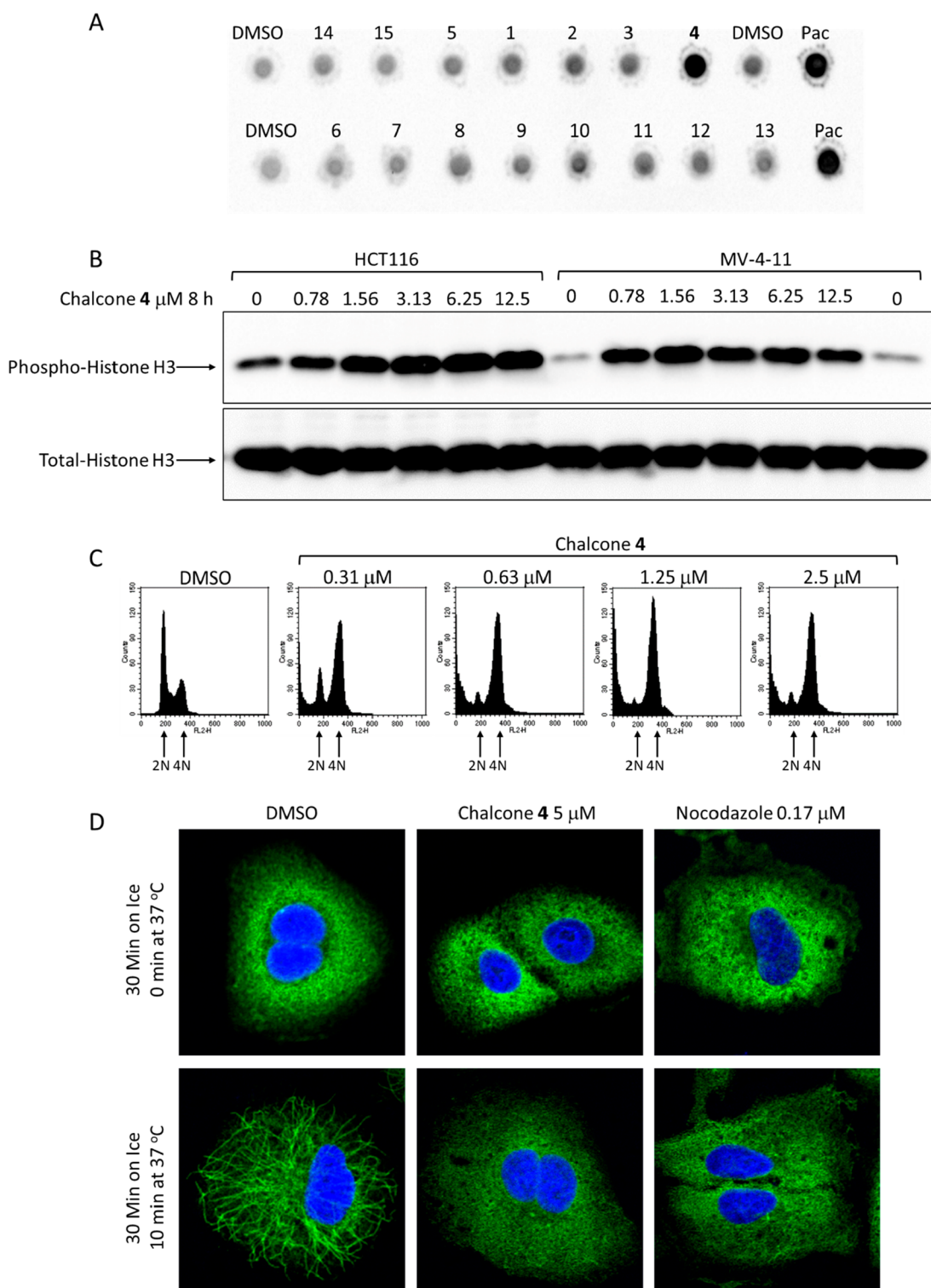


Figure 2. Chalcone 4 induces mitotic arrest and inhibits tubulin polymerization in cells. (A) Dot-blot assay for histone H3 phosphorylation at S10 following treatment with 25 μM for 8 h. DMSO and paclitaxel were used as a solvent and positive control, respectively (B) Chalcone 4 induces histone H3 phosphorylation at S10 in HCT116 and MV-4-11 cells. Cells were treated with the indicated concentrations of chalcone 4 for 8 h and analyzed for histone H3 phosphorylation using Western blotting. (C) MV-4-11 cells were treated with the indicated concentrations of chalcone 4 and analyzed for histone H3 phosphorylation at S10 through FACS following propidium iodide staining. (D) Chalcone 4 inhibits microtubule repolymerization in cells. Cells treated with DMSO, chalcone 4, or nocodazole were incubated on ice for 30 min followed by incubation at 37 $^{\circ}\text{C}$ for 10 min. Microtubules were analyzed through immunofluorescence using anti-tubulin antibodies.

relative selectivity of chalcones 2 and 3 toward AML cell lines containing FLT3-ITD mutation ($\text{GI}_{50} > 10 \mu\text{M}$) compared to the THP-1 cell line, which contains WT FLT3 ($\text{GI}_{50} > 100$

μM). On the other hand, the 2'-allyloxy derivative of natural chalcone 3, viz., chalcone 4, was the most selective and potent of the four chalcones toward FLT3-ITD cell lines, with GI_{50}

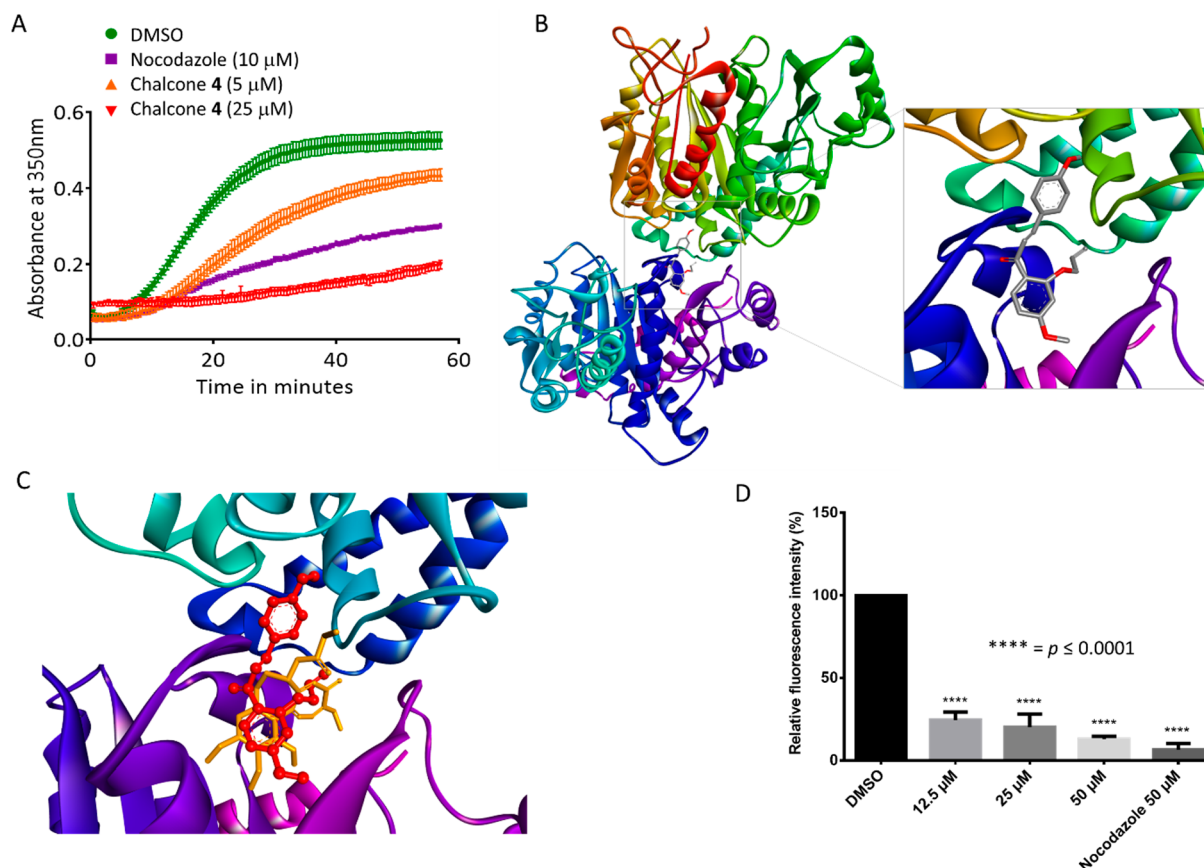


Figure 3. Chalcone 4 is a microtubule polymerization inhibitor. (A) Chalcone 4 inhibits tubulin polymerization in a biochemical assay. The polymerization assay was performed with purified tubulin in the presence of DMSO, chalcone 4 (5 and 25 μM), and nocodazole (10 μM). (B) Docking of chalcone 4 in the colchicine-binding site of tubulin. (C) Overlap of chalcone 4 (red) and colchicine (orange) in the colchicine-binding cavity of tubulin. (D) Colchicine displacement by chalcone 4. Increasing concentrations of chalcone 4 were incubated with tubulin in the presence of 20 μM colchicine, and the fluorescence intensity was measured on a plate reader. The graph represents fluorescence intensity relative to the DMSO control.

values ranging from 0.20 to 0.24 μM (Table 1). Interestingly, the allyloxy group at C-2' of chalcone 4 dramatically enhanced the activity toward MOLM-13 (>130-fold), MV-4-11 (>160-fold), and THP-1 (>45-fold) cells, when compared with the activity of the parent natural product 3.

The selectivity of these chalcones, particularly of chalcone 4 (>20 fold selective), for the FLT3-ITD cells compared to FLT3-WT cells, indicated that they might interfere with oncogenic FLT3 signaling in FLT3-ITD cells. It was therefore determined whether these compounds could inhibit FLT3 signaling in these cells by measuring the phosphorylation of Erk, Stat5, or both. Treatment of MV-4-11 cells with all four compounds resulted in reduced phosphorylation of Stat5 and/or Erk, two key downstream targets of FLT3 (Figure 1 and Figure S2, Supporting Information). In line with its potency and selectivity in FLT3-ITD cell lines, chalcone 4 was more robust at inhibiting the phosphorylation of both Stat5 and Erk (Figure 1A).

Inhibition of two signaling proteins downstream of FLT3-ITD indicated that chalcone 4 might inhibit FLT3, a common activator upstream of both these proteins. Thus, docking of chalcone 4 with FLT3 using AutoDock Vina was investigated, and the computational outcome was analyzed for the plausible binding modes using Discovery Studio Visualizer. Chalcone 4 was found to interact with Val624 through a pi-sigma interaction and, more importantly, with Phe691 and Phe830

through pi-stacking. The binding mode also placed the carbonyl group of the chalcone 4 in a position to have a conventional hydrogen bond with Lys644. Chalcone 4 binds to the same region as tyrosine kinase inhibitor (TKI) quizartinib through interactions with the "gatekeeper" residue Phe691 and the DFG motif residue Phe830. Thus, it seems plausible to assume that chalcone 4 may act by controlling access to an allosteric pocket adjacent to the ATP-binding site (Figure 1B). The docking predictions were confirmed through direct inhibition of FLT3 by chalcone 4 in a biochemical kinase assay (Figure 1C). Chalcone 4 inhibited FLT3 with an IC_{50} value of 5.7 μM in the presence of 10 μM ATP. Two other compounds, chalcone 1 and chalcone 2, were also evaluated in this kinase assay. Chalcone 2 inhibited FLT3 with an IC_{50} value of 13.8 μM , while chalcone 1 inhibited FLT3 by 39.5% at a 100 μM concentration (Figure S3, Supporting Information). The biochemical IC_{50} value of chalcone 4, however, was significantly higher than its GI_{50} in FLT3-ITD cells. Although chalcone 4 inhibited FLT3 signaling more potently in MV-4-11 cells than FLT3 activity in a biochemical assay (IC_{50} value of 5.7 μM ; Figure 1A), the GI_{50} value of 244 nM in MV-4-11 cells suggested inhibition of a possible additional target.

Chalcone 4 Inhibits Microtubule Polymerization. In addition to the screening in leukemia cell lines, screening of the chalcones for mitotic induction (histone H3 phosphorylation at S10) in a colon carcinoma cell line (HCT116) using a dot-

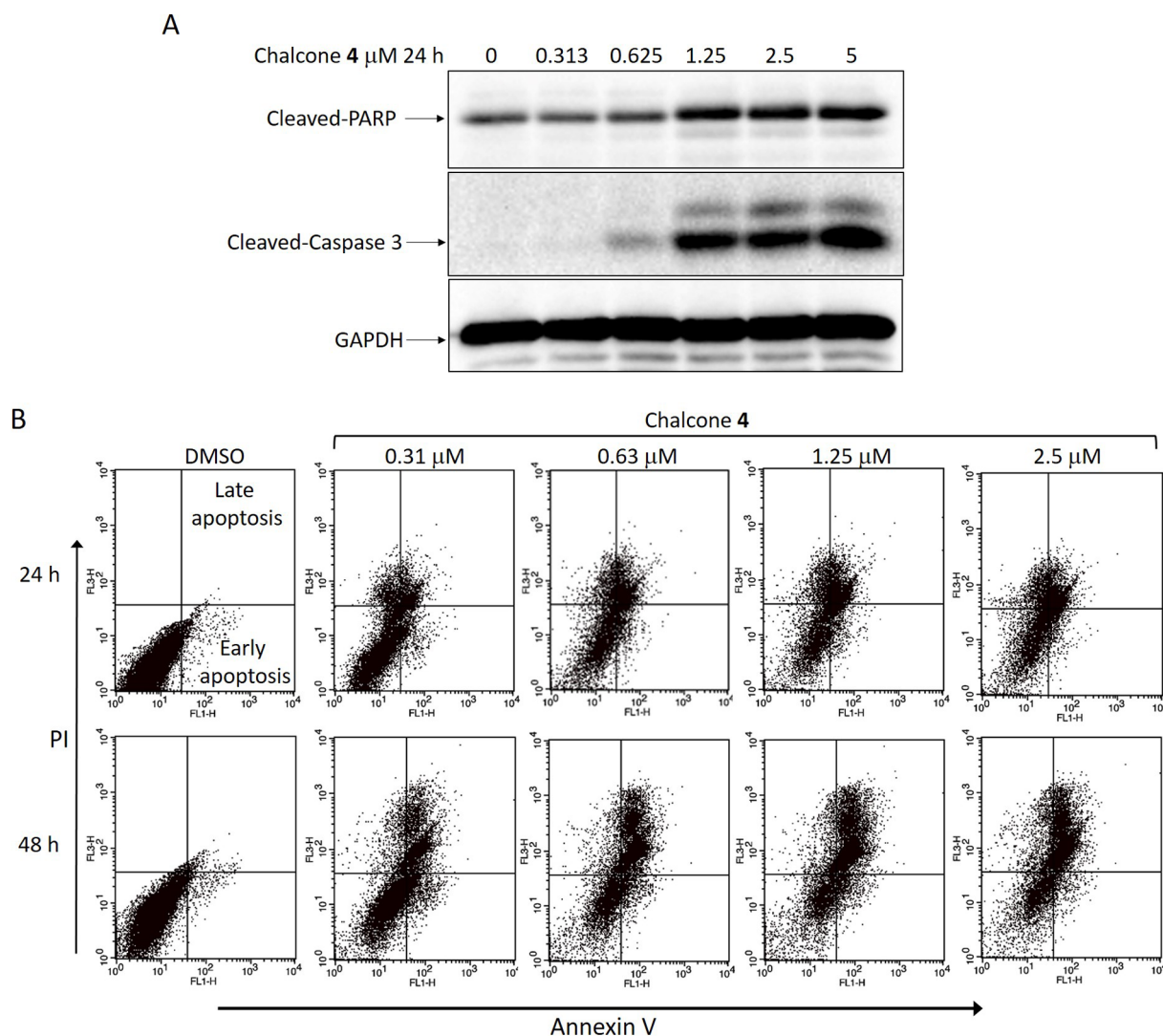


Figure 4. Chalcone 4 induces apoptosis in MV-4-11 cells. (A) Chalcone 4 causes caspase-3 and PARP cleavage. Cells were treated with the indicated concentration of the inhibitor for 24 h, and caspase-3/PARP cleavage was analyzed through Western blotting. (B) Chalcone 4 increase annexin V binding and propidium iodide uptake. Cells were treated with the indicated concentrations of chalcone 4 for 24 or 48 h and fixed and stained with FITC-annexin V/PI. Stained cells were then analyzed through FACS.

blot assay was performed. As shown in Figure 2A, chalcone 4 was a robust inducer of histone H3 phosphorylation at S10 following an 8 h treatment at a 25 μM concentration.

Treatment of HCT116 cells or MV-4-11 cells with different concentrations of chalcone 4 for 8 h caused a strong increase in histone H3 phosphorylation at S10 even at the lowest tested concentration of 0.78 μM (Figure 2B). Induction of mitotic arrest following treatment with chalcone 4 was also confirmed through FACS analysis following treatment of MV-4-11 cells with different concentrations of chalcone 4 for 24 h (Figure 2C). Induction of mitotic arrest is often a consequence of interference with microtubule dynamics. Therefore, the effect of chalcone 4 on microtubule polymerization was determined through an immunofluorescence-based assay in A549 cells. Treatment of cells with 5 μM chalcone 4 resulted in complete inhibition of microtubule repolymerization following cold-induced microtubule depolymerization (Figure 2D). Cells treated with the solvent control DMSO were able to completely repolymerize their microtubules following incubation at 37 $^{\circ}\text{C}$, while microtubules in nocodazole-treated cells remained depolymerized (Figure 2D).

In order to confirm that chalcone 4 indeed binds to and inhibits microtubule polymerization, its effect in a biochemical assay using purified tubulin was determined. As shown in Figure 3A, chalcone 4 inhibited microtubule polymerization in a dose-dependent manner (at 5 and 25 μM concentrations). DMSO was used as solvent control, while nocodazole (10 μM) was used as a positive control for depolymerization (Figure 3A). Docking studies of chalcone 4 with tubulin subsequently were performed. Tubulin has three binding sites, viz., the paclitaxel-binding site, the vinca alkaloid-binding site, and the colchicine-binding site. Polymerization inhibitors like colchicine bind at the colchicine-binding site. In agreement with the bioassays used, the docking predicted that chalcone 4 binds to tubulin at the colchicine-binding site, with one of the aromatic rings occupying the same region as occupied by the trimethoxyphenyl ring of colchicine (Figure 3B and C). Chalcone 4 undergoes two hydrogen bond interactions with the tubulin at the Leu255 and Cys241 residues. The phenyl ring adjacent to the carbonyl group shows pi-sigma interaction with Leu248, while the other aromatic ring interacts with the Ala180 and Lys 254 residues. The docking

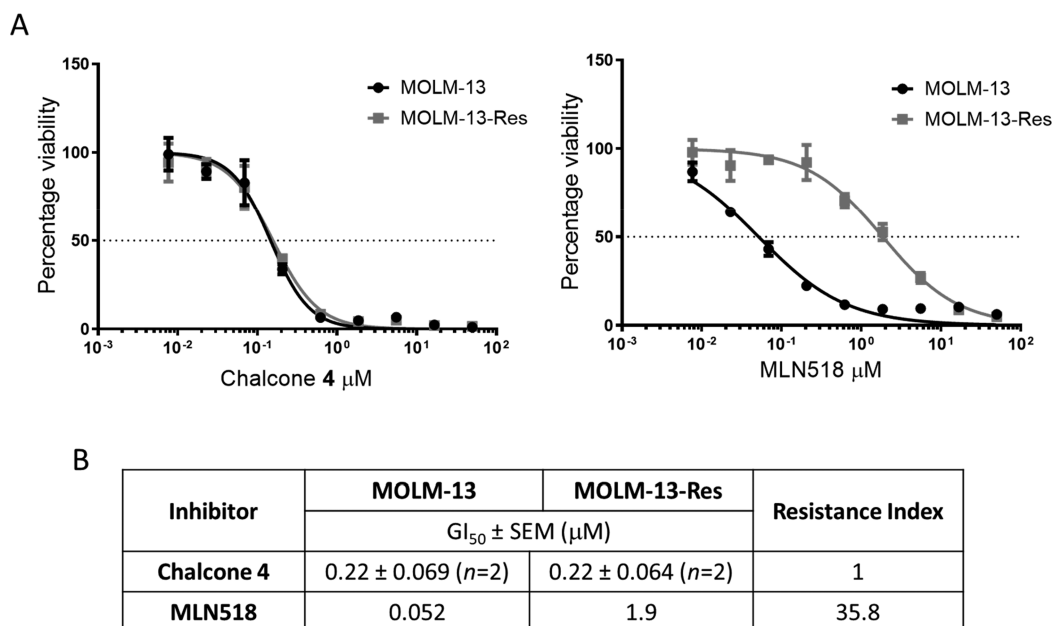


Figure 5. Chalcone 4 overcomes TKD-mediated resistance to FLT3 inhibitors. (A) GI₅₀ graphs for chalcone 4 and MLN518 in MOLM-13 and MOLM-13-Res cell lines in a three-day MTS proliferation assay. (B) Table summarizing the GI₅₀ values and fold resistance of two inhibitors using the MOLM-13 and MOLM-13-Res cell lines.

prediction for association with the colchicine-binding site was confirmed through a colchicine displacement assay. Chalcone 4 was able to displace colchicine significantly at all three concentrations used (Figure 3D) with 75%, 80%, and 87% colchicine displacement at 12.5, 25, and 50 μM, respectively. The positive control, nocodazole, caused 93.5% displacement at a 50 μM concentration in the same assay (Figure 3D).

Chalcone 4 Induces Apoptosis in MV-4-11 Cells. Next, the ability of chalcone 4 to induce apoptosis in MV-4-11 cells was determined through analysis of activation of caspase-3, an executioner caspase, or expression of an apoptotic marker, phosphatidylserine, on the cell surface. Treatment of MV-4-11 cells with different concentrations of chalcone 4 (0.313, 0.625, 1.25, 2.5, and 5 μM) for 24 h resulted in increased cleavage of caspase 3, indicating its activation (Figure 4A). Cleavage of caspase-3 was accompanied by cleavage of poly(ADP-ribose) polymerase (PARP), a substrate of caspase-3. Similarly, treatment of MV-4-11 cells with different concentrations of chalcone 4 for 24 and 48 h induced annexin V binding and propidium iodide retention, indicating early and late apoptotic cell death (Figure 4B).

Chalcone 4 Overcomes FLT3-TKD-Mediated Resistance. Considering that chalcone 4 could inhibit tubulin polymerization in addition to inhibiting FLT3, its ability to overcome D835Y-mediated resistance to FLT3 inhibitors was evaluated using the MOLM-13 and MOLM-13-Res (with D835Y mutation) cell lines. Parental MOLM-13 cells were sensitive to MLN518 (tandutinib) with a GI₅₀ value of 52 nM (Figure 5). MOLM-13-Res cells, generated through incubation with increasing concentrations of MLN518,²⁶ were, however, resistant to MLN518 with a GI₅₀ value of 1.9 μM (36-fold resistant). Chalcone 4, on the contrary, was equally potent in MOLM-13 and MOLM-13-Res cell lines with a GI₅₀ value of 0.22 μM in both the cell lines (Figure 5). This shows that chalcone 4 can inhibit the growth of MOLM-13 cells irrespective of the TKD mutation status, probably because of its dual inhibition of FLT3 and microtubule polymerization.

Privileged scaffolds have a wide range of applications in medicinal chemistry for drug discovery. The flavonoid subtype chalcone is considered as a privileged scaffold and is present in numerous natural products.³⁵ Both natural and synthetic chalcones have illustrated many interesting biological activities with potential clinical applications for various diseases, including cancer.^{35,36,42} Some chalcone derivatives, for example, have demonstrated promising activity toward T-cell acute lymphoblastic leukemia (T-ALL)^{43,44} and CML⁴⁵ cell lines.

Dependence of cancer cells on the activity of a single oncogene (oncogene addiction) makes them sensitive to inhibition of that oncogene or its downstream signaling pathway.⁴⁶ Chronic myeloid leukemia (CML) cells, for example, are dependent on the BCR-ABL oncogene, and their dependence on the constitutive activity of ABL kinase has been successfully exploited for the treatment of CML.⁴⁷ Similarly, the reliance of a subset of AML cells on constitutive activation of FLT3 for proliferation and survival makes them sensitive to FLT3 inhibition, as discussed above.²² The oncogenic dependence of MV-4-11 and K-562 cell lines to FLT3-ITD and BCR-ABL, respectively, was exploited for screening the chalcone library. Differential antiproliferative activity of chalcones in one or the other cell line was used as an indicator of interference with the signaling through FLT3-ITD or BCR-ABL oncogenes. As a consequence, chalcone 4 was identified as being more active in FLT3-ITD cells, where it inhibited the phosphorylation of two of the downstream targets of activated FLT3, STAT5 and ERK.

Actively dividing cancer cells are known to elude apoptosis, which is why diverse anticancer drugs work by ultimately promoting apoptotic cell death through related mechanisms.⁴⁸ Caspase 3, a cysteine protease, is an important factor in executing the apoptotic process. Once activated through cleavage, it proteolytically cleaves downstream substrates such as PARP.⁴⁹ Mitotic arrest induced by microtubule-targeting agents activates the spindle assembly checkpoint and

eventually leads to apoptotic cell death.⁵⁰ FLT3 inhibitors also prevent proliferation by triggering cell cycle arrest and inducing apoptosis.⁶ Chalcone 4, which inhibits both microtubule polymerization and oncogenic FLT3 signaling in MV-4-11 cells, induced apoptotic cell death in these cells as determined by various methods including increased caspase 3 and PARP cleavage as well as annexin V binding and propidium iodide uptake.

Combinations of FLT3 inhibitors with chemotherapeutic or targeted drugs have been used in the clinic for enhanced efficacy and to overcome resistance to FLT3 inhibitors.^{22,51} Despite their advantages, fully elucidating clinical benefits with combination can be challenging, considering the pharmacokinetic differences such as drug–drug interactions.⁵² Use of multitarget monotherapies (polypharmacology) provides an alternative to drug combinations,⁵³ and many small molecule inhibitors with numerous targets in addition to FLT3 have been reported to overcome TKD-mediated resistance to FLT3 inhibitors.²³ Examples include dual inhibitors of FLT3/CDK4 (AMG 925),⁵⁴ FLT3/JAK2 (pacritinib),⁵⁵ and FLT3/Aurora (CCT137690).²⁶ Similarly, some kinase inhibitors have shown microtubule depolymerizing activity, which could contribute to their enhanced efficacy and ability to evade acquisition of drug resistance.⁵⁶ A microtubule polymerization inhibitor with activity against multiple kinases, including FLT3, has been shown to inhibit proliferation and induce apoptosis in cancer cell lines of various origins including leukemia.⁵⁴ Chalcone 4 identified in this study represents a promising lead for targeting a subset of AML as a single agent. Further lead optimization, selectivity, and pharmacokinetic studies are required for in vivo evaluation of chalcone 4.

EXPERIMENTAL SECTION

General Experimental Procedures. Melting points were measured on a Yanaco MP-J3 model melting point apparatus. The NMR spectra were recorded using an Avance 500 MHz spectrometer (Bruker, Billerica, MA, USA) or Agilent DD2 400 system (Agilent Technologies, USA). Chemical shifts are reported in ppm (δ). Coupling constants, J , are reported in Hz. HRESIMS were obtained on a Thermo Fischer LTQ Orbitrap Elite mass spectrometer, while elemental analyses were recorded on an Elementar Vario EL CHNS-O elemental analyzer. Column chromatography was performed on Sephadex LH 20 (Fluka, Germany), silica gel (0.040–0.063 mm, Merck, Germany), and silica gel 60 silanized (0.063–0.200 mm, Merck, Germany), whereas analytical TLC was performed on precoated silica gel F 254 aluminum sheets (Merck, Germany). Yields refer to chromatographically and spectroscopically pure compounds unless otherwise stated. All reagents and solvents were purchased from commercial sources unless otherwise specified.

General Procedure for the Synthesis of Chalcones 1–3. A mixture of equimolar amounts of acetophenones, viz., 1-(2-hydroxyphenyl)ethanone or 2-hydroxy-4-methoxyacetophenone, and benzaldehydes, such as benzaldehyde, 3,4-dimethoxybenzaldehyde, or 4-methoxybenzaldehyde, in 25 mL of EtOH was heated at 50 °C. After the addition of 50% aqueous NaOH (6 mL) solution, the mixture was further stirred at 50 °C for 5 h. Then, the reaction mixture was stirred at room temperature for 24 h, and a yellow precipitate was formed. Furthermore, each mixture was diluted with ice-cold water (150 mL) and then acidified with diluted HCl (20 mL). Finally, the resulting precipitates formed were filtered off, dried, and crystallized with aqueous ethanol to afford the desired chalcone.

2'-Hydroxychalcone (1). Chalcone 1 was prepared according to a general procedure, and spectroscopic data were in good agreement with previously published data.⁵⁷ ¹H NMR (500 MHz, CDCl₃) δ 6.95 (1H, m), 7.04 (1H, dd, J = 1.5, 8.0 Hz), 7.04 (1H, dd, J = 1.5, 8.0 Hz), 7.49 (3H, m), 7.51 (1H, m), 7.67 (3H, m), 7.95 (2H, m), 12.81

(1H, s, OH); ESIMS m/z 247.1 [M + Na]⁺, C₁₅H₁₂NaO₂; anal. calcd for C₁₅H₁₂O₂, C 80.34, H 5.39; found: C, 80.27, H 5.33.

3,4,4'-Trimethoxy-2'-hydroxychalcone (2). Chalcone 2 was prepared according to a general procedure, and spectroscopic data were in good agreement with previously published data:⁵⁸ mp 159 °C; ¹H NMR (500 MHz, CDCl₃) δ 3.88 (3H, s), 3.96 (3H, s), 3.98 (3H, s), 6.50 (2H, m), 6.92 (1H, d, J = 8.4 Hz), 7.16 (1H, bs), 7.26 (1H, d, J = 1.6 Hz), 7.45 (1H, d, J = 15.6 Hz), 7.85 (1H, s), 7.87 (1H, d, J = 15.6 Hz), 13.54 (1H, s, OH-2'); ESIMS m/z 336.9 [M + Na]⁺, C₁₈H₁₈NaO₅; anal. calcd for C₁₈H₁₈O₅, C 68.78, H 5.77; found: C 68.74, H 5.71.

4,4'-Dimethoxy-2'-hydroxychalcone (3). Chalcone 3 was prepared according to a general procedure, and spectroscopic data were in good agreement with previously published data:⁵⁹ mp 91–93 °C; ¹H NMR (500 MHz, CDCl₃) δ 3.86 (3H, s, OCH₃), 3.87 (3H, s, OCH₃), 6.49–6.47 (2H, m, H-5', H-3'), 6.95 (1H, d, J = 8.8 Hz, H-5), 7.48 (1H, d, J = 15.9 Hz, H- α), 7.62 (2H, d, J = 8.8 Hz, H-2, H-6), 7.85 (1H, d, J = 8.8, H-6'), 7.88 (1H, d, J = 15.9 Hz, H- β), 13.54 (1H, s, OH-2'); ESIMS m/z 307.3 [M + Na]⁺, C₁₇H₁₆NaO₄; anal. calcd for C₁₇H₁₆O₄, C 71.82, H 5.67; found: C 71.79, H 5.64.

2'-Allyloxy-4,4'-dimethoxychalcone (4). A mixture of chalcone 3 (2.00 g, 7.00 mmol), allyl bromide (1.27 g, 1 mL, 10.50 mmol), and 40% potassium fluoride alumina (5.00 g, 35.00 mmol of KF) in 25 mL of CH₃CN (20 mL) was stirred magnetically at room temperature for 4 h. The solid material was filtered and washed with CH₂Cl₂. The filtrate was concentrated under reduced pressure to afford a yellow residue. Purification of the residue was done by flash chromatography using petroleum ether–ethyl acetate (5:1) to afford a yellow solid of chalcone 4 in 85% yield: ¹H NMR (400 MHz, CDCl₃) δ 3.85 (3H, s, OCH₃), 3.86 (3H, s, OCH₃), 4.62 (2H, dd, J = 5.0, 1.0 Hz, CH₂–allyl), 5.28 (1H, dd, J = 10.3, 1.3 Hz, allyl), 5.47 (1H, d, J = 17.3, 1.3, allyl), 6.07 (1H, m, allyl), 6.48 (1H, d, J = 1.3 Hz, H-3'), 6.58 (1H, dd, J = 8.0, 1.3 Hz, H-5'), 6.91 (2H, d, J = 8.7 Hz, H-3, H-5), 7.46 (1H, d, J = 16.0 Hz, H- α), 7.78 (1H, d, J = 8.0 Hz, H-6'), 7.68 (1H, d, J = 16.0 Hz, H- β), 7.78 (2H, d, J = 8.7 Hz, H-2, H-6); ¹³C NMR (100 MHz, CDCl₃) δ 55.3 (OCH₃), 55.5 (OCH₃), 69.4 (allyl), 99.8 (C-3'), 105.5 (C-5'), 114.2 (C-3, C-5), 117.8 (C-3), 122.8 (C- α), 125.1 (C-1'), 128.1 (C-2), 129.7 (C-2, C-4), 132.4 (C-1), 133.8 (C-6'), 141.6 (C- β), 159.2 (C-4), 161.1 (C-2'), 164.8 (C-4'), 190.4 (CO); HRESIMS m/z [M + H]⁺ 325.1415 (calcd for C₂₀H₂₁O₄, 325.1434); anal. calcd for C₂₀H₂₀O₄, C 74.06, H 6.22; found: C 74.03, H 6.19.

General Procedure for the Synthesis of Chalcones 6–15. The chemistry of chalcones 6–15 was already published by our group.³⁶ A mixture of equimolar amounts of appropriate acetophenones and benzaldehydes was added to a round-bottom flask in 25 mL of EtOH. Then a 15 N ethanolic solution of sodium ethoxide (0.2 mL) was added to the reaction mixture, and the reaction mixture was stirred overnight (15–17 h) at room temperature. Then the solvent was removed, and the mixture was dissolved in ethyl acetate. The contents of the flask were then transferred to the separating funnel and washed with brine. Then the organic layer was dried over MgSO₄, and the solvent was removed to obtain the product. In case the product was an oil, it was purified by column chromatography in EtOAc–hexanes, and in case of the solid, it was purified by recrystallization from ethanol to afford chalcones.

Cell Culture. MV-4-11, MOLM-13, MOLM-13-Res (provided by Dr. Spiros Linardopoulos, Institute of Cancer Research, London, UK), K-562, and THP-1 were cultured in Roswell Park Memorial Institute (RPMI) medium, while HCT116 and A549 cells were cultured in DMEM (Dulbecco's modified Eagle's medium). Both media were supplemented with 10% fetal bovine serum (FBS) and 5% antibiotic–antimycotic. All the cell lines in their respective supplemented medium were cultured at 37 °C in humidified incubators with 5% CO₂.

Cell Proliferation Assay. Effect of compounds on the proliferation of cells was measured through a colorimetric MTS cell proliferation assay. For initial screening, 15 000 cells (MV-4-11 and K562) were split per well in 96-well plates, treated with 25 and 50 μ M concentrations of the compounds, and incubated at 37 °C for 72 h. At

the end of treatment, 20 μL of MTS solution was added to each well, and the plates were again incubated at 37 °C for 3 h. Optical density (OD) was then measured at 490 nm on a microplate reader. Percentage inhibition was calculated, and graphs were made in Excel. For GI_{50} determinations, 15 000 cells per well in 96-well plates were treated with nine 2-fold dilutions of the inhibitors (starting with 50 μM) and incubated at 37 °C for 72 h. At the end of the treatment, the MTS assay was performed as described above, and the GI_{50} values were calculated using GraphPad Prism.

Immunoblotting. Cells treated with the indicated concentrations of chalcone 4 for 8 or 24 h were collected in lysis buffer (25 mM Tris pH 7.4, 1% Triton X-100, 50 mM sodium chloride supplemented with protease and phosphatase inhibitors) through incubation on ice for 10 min. Cell lysates were sonicated and cleared by centrifugation at 13600g for 10 min. Protein concentrations of the cleared cell lysates were measured, and equal amounts of proteins were used for preparing the samples for SDS-PAGE. Samples were run on 10% SDS-PAGE, and separated proteins were transferred onto nitrocellulose membranes. Membranes were blocked with 5% skimmed milk and incubated overnight at 4 °C with the primary antibodies. The next day, membranes were washed with PBS containing 0.1% Tween (PBST) and incubated with HRP-labeled secondary antibodies for 1 h at room temperature. The membranes were washed again, developed with the ECL reagent, and imaged using ChemiDoc. Antibodies for Stat5, P-Stat5, cleaved PARP, and cleaved caspase 3 were from Cell Signaling Technology (CST). Antibodies for P-histone H3 (S10) and alpha tubulin were from Abcam, P-Erk and GAPDH were from Santa Cruz, and T-histone H3 were from Southern Biotech.

Microtubule Repolymerization Assay. For the immunofluorescence-based microtubule repolymerization assay, A549 cells were plated on P-L-lysine-coated coverslips in six-well plates. Cells were treated (in two sets) with the different concentrations of inhibitors or DMSO control and incubated on ice for 30 min for microtubule depolymerization. One set of cells was fixed with ice-cold methanol, and the other set was then shifted to 37 °C for 10 min to allow repolymerization of the microtubules followed by fixation with ice-cold methanol. Fixed cells were blocked with 2% BSA (in PBS) and incubated with alpha-tubulin antibodies (1:500) for 1 h. Coverslips were washed with PBS and incubated with FITC-labeled anti-mouse antibodies (1:500) for 1 h in the dark. Cells were washed five times in PBS and stained with DAPI (1:10000 dilution) during the penultimate wash. Stained coverslips were then mounted onto glass slides with Fluoromount and imaged using a Nikon confocal microscope.

Cell Cycle and Apoptosis Assay. For the cell cycle analysis, cells were treated with different concentrations of chalcone 4 for 8 h, collected through trypsinization, and fixed with 85% ice-cold ethanol. Fixed cells were washed with PBS containing 1% FBS and stained with a propidium iodide/RNase solution for 30 min at 37 °C. Cells were analyzed with a BD FACSCalibur instrument. For the apoptosis assay, cells were treated with different concentration of chalcone 4 for 24 and 48 h. Cells were then collected and stained with an annexin V/PI apoptosis kit (Santa Cruz) according to the manufacturer's instructions. Stained samples were then analyzed with the BD FACSCalibur instrument.

Dot-Blot Screening. For dot-blot screening, 50 000 HCT116 cells per well were split in a 96-well plate on day 1. The next day, cells were treated with 25 μM concentrations of the test compounds for 8 h. Cells were then lysed by adding 40 μL of 2 \times SDS sample buffer containing 200 mM dithiothreitol (DTT). Cells in each well were sonicated for 5 s followed by incubation of the plate on a hot-plate for 10 min. The following day, 2.5 μL of the samples was blotted on nitrocellulose membranes and dried for 20 min and then washed once with PBST for 2 min. The membranes were blocked in 5% milk. Anti-phospho-histone H3 antibody (1:500 dilution) was added and incubated overnight at 4 °C. The membranes were given three 5 min washes with PBST, then incubated with the anti-rabbit secondary antibody (1:1000 dilution, Southern Biotech) for 1 h at room

temperature. Membranes were developed with ECL reagent on Chemidoc (Bio-Rad).

In Vitro Assays. Both an in vitro tubulin polymerization assay and a colchicine displacement assay were performed by Ecrins Therapeutics (France), as described elsewhere.⁶⁰ The FLT3 kinase assay was carried out by SelectScreen Kinase Profiling Services (ThermoFisher).

Docking Studies. AutoDock Tools (ADT, The Scripps Research Institute, La Jolla, CA, USA) was used to perform the docking. The crystal structure of FLT3 was obtained from Protein Data Bank (PDB code: 4rt7). It was prepared for docking by removing the ligand. The addition of hydrogen atoms was performed using MGLTools for AutoDock, and the docking was performed at an exhaustiveness of 8 and grid box dimensions of 40, 40, 40. The docking for tubulin was performed as described by Manzoor et al.⁶⁰ Analysis of the docking was done by checking the interaction energy, clustering, and the conformation of the protein and ligand using PyMol and Discovery Studio Visualizer.

■ ASSOCIATED CONTENT

Supporting Information

The Supporting Information is available free of charge at <https://pubs.acs.org/doi/10.1021/acs.jnatprod.0c00699>.

Supplementary figures and detailed NMR data (PDF)

■ AUTHOR INFORMATION

Corresponding Authors

Amir Faisal – Department of Biology, Syed Babar Ali School of Science and Engineering, Lahore University of Management Sciences, Lahore, Pakistan; orcid.org/0000-0002-7376-8286; Phone: +92-423-560-8453; Email: amir.faisal@lums.edu.pk

Hidayat Hussain – Department of Chemistry, University of Paderborn, 33098 Paderborn, Germany; Department of Bioorganic Chemistry, Leibniz Institute of Plant Biochemistry, D-06120 Halle (Saale), Germany; orcid.org/0000-0002-8654-8127; Email: hussainchem3@gmail.com, Hidayat.Hussain@ipb-halle.de

Authors

Haleema Sadia Malik – Department of Biology, Syed Babar Ali School of Science and Engineering, Lahore University of Management Sciences, Lahore, Pakistan

Aishah Bilal – Department of Biology, Syed Babar Ali School of Science and Engineering, Lahore University of Management Sciences, Lahore, Pakistan

Rahim Ullah – Department of Biology, Syed Babar Ali School of Science and Engineering, Lahore University of Management Sciences, Lahore, Pakistan

Maheen Iqbal – Department of Biology, Syed Babar Ali School of Science and Engineering, Lahore University of Management Sciences, Lahore, Pakistan

Sardraz Khan – Department of Chemistry and Chemical Engineering, Syed Babar Ali School of Science and Engineering, Lahore University of Management Sciences, Lahore, Pakistan

Ishtiaq Ahmed – Department of Chemistry, University of Paderborn, 33098 Paderborn, Germany

Karsten Krohn – Department of Chemistry, University of Paderborn, 33098 Paderborn, Germany

Rahman Shah Zaib Saleem – Department of Chemistry and Chemical Engineering, Syed Babar Ali School of Science and Engineering, Lahore University of Management Sciences, Lahore, Pakistan; orcid.org/0000-0002-9615-4471

Complete contact information is available at:

<https://pubs.acs.org/10.1021/acs.jnatprod.0c00699>

Notes

The authors declare no competing financial interest.

ACKNOWLEDGMENTS

This research was supported by the startup grant (STG-BIO-1009) provided by Lahore University of Management Sciences (LUMS) to A.F. H.H. thanks the Alexander von Humboldt Foundation for its generous support in providing the opportunity to do research in Germany

REFERENCES

- (1) Estey, E.; Dohner, H. *Lancet* **2006**, *368*, 1894–907.
- (2) De Kouchkovsky, I.; Abdul-Hay, M. *Blood Cancer J.* **2016**, *6*, No. e441.
- (3) Berenstein, R. *Biomarker Insights* **2015**, *10*, 1–14.
- (4) Agnes, F.; Shamoan, B.; Dina, C.; Rosnet, O.; Birnbaum, D.; Galibert, F. *Gene* **1994**, *145*, 283–288.
- (5) Yamamoto, Y.; Kiyoi, H.; Nakano, Y.; Suzuki, R.; Kodera, Y.; Miyawaki, S.; Asou, N.; Kuriyama, K.; Yagasaki, F.; Shimazaki, C.; Akiyama, H.; Saito, K.; Nishimura, M.; Motoji, T.; Shinagawa, K.; Takeshita, A.; Saito, H.; Ueda, R.; Ohno, R.; Naoe, T. *Blood* **2001**, *97*, 2434–2439.
- (6) Levis, M.; Small, D. *Leukemia* **2003**, *17*, 1738–1752.
- (7) Abu-Duhier, F. M.; Goodeve, A. C.; Wilson, G. A.; Care, R. S.; Peake, I. R.; Reilly, J. T. *Br. J. Haematol.* **2001**, *113*, 1076–1077.
- (8) Kiyoi, H.; Towatari, M.; Yokota, S.; Hamaguchi, M.; Ohno, R.; Saito, H.; Naoe, T. *Leukemia* **1998**, *12*, 1333–1337.
- (9) Leung, A. Y.; Man, C. H.; Kwong, Y. L. *Leukemia* **2013**, *27*, 260–268.
- (10) Mizuki, M.; Fenski, R.; Halfter, H.; Matsumura, I.; Schmidt, R.; Muller, C.; Gruning, W.; Kratz-Albers, K.; Serve, S.; Steur, C.; Buchner, T.; Kienast, J.; Kanakura, Y.; Berdel, W. E.; Serve, H. *Blood* **2000**, *96*, 3907–3914.
- (11) Brandts, C. H.; Sargin, B.; Rode, M.; Biermann, C.; Lindtner, B.; Schwable, J.; Buerger, H.; Muller-Tidow, C.; Choudhary, C.; McMahon, M.; Berdel, W. E.; Serve, H. *Cancer Res.* **2005**, *65*, 9643–9650.
- (12) Lee, S. H.; Paietta, E.; Racevskis, J.; Wiernik, P. H. *Am. J. Hematol.* **2009**, *84*, 701–702.
- (13) Smith, B. D.; Levis, M.; Beran, M.; Giles, F.; Kantarjian, H.; Berg, K.; Murphy, K. M.; Dausess, T.; Allebach, J.; Small, D. *Blood* **2004**, *103*, 3669–3676.
- (14) Zarrinkar, P. P.; Gunawardane, R. N.; Cramer, M. D.; Gardner, M. F.; Brigham, D.; Belli, B.; Karaman, M. W.; Pratz, K. W.; Pallares, G.; Chao, Q.; Sprankle, K. G.; Patel, H. K.; Levis, M.; Armstrong, R. C.; James, J.; Bhagwat, S. S. *Blood* **2009**, *114*, 2984–2992.
- (15) Levis, M. *Blood* **2017**, *129*, 3403–3406.
- (16) Sidaway, P. *Nat. Rev. Clin. Oncol.* **2020**, *17*, 69.
- (17) Knapper, S. *Expert Opin. Invest. Drugs* **2011**, *20*, 1377–1395.
- (18) Grunwald, M. R.; Levis, M. J. *Int. J. Hematol.* **2013**, *97*, 683–694.
- (19) Chu, S. H.; Small, D. *Drug Resist. Updates* **2009**, *12*, 8–16.
- (20) Smith, C. C.; Wang, Q.; Chin, C. S.; Salerno, S.; Damon, L. E.; Levis, M. J.; Perl, A. E.; Travers, K. J.; Wang, S.; Hunt, J. P.; Zarrinkar, P. P.; Schadt, E. E.; Kasarskis, A.; Kuriyan, J.; Shah, N. P. *Nature* **2012**, *485*, 260–263.
- (21) Man, C. H.; Fung, T. K.; Ho, C.; Han, H. H.; Chow, H. C.; Ma, A. C.; Choi, W. W.; Lok, S.; Cheung, A. M.; Eaves, C.; Kwong, Y. L.; Leung, A. Y. *Blood* **2012**, *119*, 5133–5143.
- (22) Daver, N.; Schlenk, R. F.; Russell, N. H.; Levis, M. J. *Leukemia* **2019**, *33*, 299–312.
- (23) Yuan, T.; Qi, B.; Jiang, Z.; Dong, W.; Zhong, L.; Bai, L.; Tong, R.; Yu, J.; Shi, J. *Eur. J. Med. Chem.* **2019**, *178*, 468–483.
- (24) Stone, R. M.; Mandrekar, S. J.; Sanford, B. L.; Laumann, K.; Geyer, S.; Bloomfield, C. D.; Thiede, C.; Prior, T. W.; Dohner, K.; Marcucci, G.; Lo-Coco, F.; Klisovic, R. B.; Wei, A.; Sierra, J.; Sanz, M. A.; Brandwein, J. M.; Witte, T.; Niederwieser, D.; Appelbaum, F. R.; Medeiros, B. C.; Tallman, M. S.; Krauter, J.; Schlenk, R. F.; Ganser, A.; Serve, H.; Ehninger, G.; Amadori, S.; Larson, R. A.; Dohner, H. N. *Engl. J. Med.* **2017**, *377*, 454–464.
- (25) Larrosa-Garcia, M.; Baer, M. R. *Mol. Cancer Ther.* **2017**, *16*, 991–1001.
- (26) Moore, A. S.; Faisal, A.; Gonzalez de Castro, D.; Bavetsias, V.; Sun, C.; Atrash, B.; Valenti, M.; de Haven Brandon, A.; Avery, S.; Mair, D.; Mirabella, F.; Swansbury, J.; Pearson, A. D.; Workman, P.; Blagg, J.; Raynaud, F. I.; Eccles, S. A.; Linardopoulos, S. *Leukemia* **2012**, *26*, 1462–1470.
- (27) Bavetsias, V.; Crumpler, S.; Sun, C.; Avery, S.; Atrash, B.; Faisal, A.; Moore, A. S.; Kosmopoulou, M.; Brown, N.; Sheldrake, P. W.; Bush, K.; Henley, A.; Box, G.; Valenti, M.; de Haven Brandon, A.; Raynaud, F. I.; Workman, P.; Eccles, S. A.; Bayliss, R.; Linardopoulos, S.; Blagg, J. *J. Med. Chem.* **2012**, *55*, 8721–8734.
- (28) Brouhard, G. J.; Rice, L. M. *Nat. Rev. Mol. Cell Biol.* **2018**, *19*, 451–463.
- (29) Wilson, L.; Jordan, M. A. *J. Chemother.* **2004**, *16*, 83–85.
- (30) Dumontet, C.; Jordan, M. A. *Nat. Rev. Drug Discov.* **2010**, *9*, 790–803.
- (31) Munshi, N.; Jeay, S.; Li, Y.; Chen, C. R.; France, D. S.; Ashwell, M. A.; Hill, J.; Moussa, M. M.; Leggett, D. S.; Li, C. J. *Mol. Cancer Ther.* **2010**, *9*, 1544–1553.
- (32) Basilico, C.; Pennacchietti, S.; Vigna, E.; Chiriaco, C.; Arena, S.; Bardelli, A.; Valdembri, D.; Serini, G.; Michieli, P. *Clin. Cancer Res.* **2013**, *19*, 2381–2392.
- (33) Aoyama, A.; Katayama, R.; Oh-Hara, T.; Sato, S.; Okuno, Y.; Fujita, N. *Mol. Cancer Ther.* **2014**, *13*, 2978–2990.
- (34) Carta, D.; Bortolozzi, R.; Hamel, E.; Basso, G.; Moro, S.; Viola, G.; Ferlin, M. G. *J. Med. Chem.* **2015**, *58*, 7991–8010.
- (35) Zhuang, C.; Zhang, W.; Sheng, C.; Zhang, W.; Xing, C.; Miao, Z. *Chem. Rev.* **2017**, *117*, 7762–7810.
- (36) Ifitkhar, S.; Khan, S.; Bilal, A.; Manzoor, S.; Abdullah, M.; Emwas, A. H.; Sioud, S.; Gao, X.; Chotana, G. A.; Faisal, A.; Saleem, R. S. *Z. Bioorg. Med. Chem. Lett.* **2017**, *27*, 4101–4106.
- (37) Ngadjui, B. T.; Kapche, G. W.; Tamboue, H.; Abegaz, B. M.; Connolly, J. D. *Phytochemistry* **1999**, *51*, 119–123.
- (38) Van-Der Krieken, S. E.; Popeijus, H. E.; Bendik, I.; Boehlendorf, B.; Konings, M. C. J. M.; Tayyeb, J.; Mensink, R. P.; Plat, J. *Lipids* **2018**, *53*, 1021–1030.
- (39) Wang, J.; Wang, N.; Yao, X.; Kitanaka, S. *Asian J. Tradit. Med.* **2007**, *2*, 23–29.
- (40) Kim, H. G.; Oh, H. J.; Ko, J. H.; Song, H. S.; Lee, Y. G.; Kang, S. C.; Lee, D. Y.; Baek, N. I. *Bioorg. Chem.* **2019**, *85*, 274–281.
- (41) Ortega, C. A.; Maria, A. O. M.; Gianello, J. C. *Molecules* **2000**, *5*, 465–467.
- (42) Riaz, S.; Iqbal, M.; Ullah, R.; Zahra, R.; Chotana, G. A.; Faisal, A.; Saleem, R. S. *Z. Bioorg. Chem.* **2019**, *87*, 123–135.
- (43) Mori, M.; Tottone, L.; Quaglio, D.; Zhdanovskaya, N.; Ingallina, C.; Fusto, M.; Ghirga, F.; Peruzzi, G.; Crestoni, M. E.; Simeoni, F.; Giulimondi, F.; Talora, C.; Botta, B.; Screpanti, I.; Palermo, R. *Sci. Rep.* **2017**, *7*, 2213.
- (44) Quaglio, D.; Zhdanovskaya, N.; Tobajas, G.; Cuartas, V.; Balducci, S.; Christodoulou, M. S.; Fabrizi, G.; Gargantilla, M.; Priego, E. M.; Pestana, A. C.; Passarella, D.; Screpanti, I.; Botta, B.; Palermo, R.; Mori, M.; Ghirga, F.; Perez-Perez, M. J. *ACS Med. Chem. Lett.* **2019**, *10*, 639–643.
- (45) Novilla, A.; Astuti, I.; Suwito, H. *J. Med. Sci.* **2017**, *49*, 153–164.
- (46) Pagliarini, R.; Shao, W.; Sellers, W. R. *EMBO Rep.* **2015**, *16*, 280–296.
- (47) An, X.; Tiwari, A. K.; Sun, Y.; Ding, P. R.; Ashby, C. R.; Chen, Z. S. *Leuk. Res.* **2010**, *34*, 1255–1268.
- (48) Lowe, S. W.; Lin, A. W. *Carcinogenesis* **2000**, *21*, 485–495.
- (49) Wolf, B. B.; Green, D. R. *J. Biol. Chem.* **1999**, *274*, 20049–20052.
- (50) Bhalla, K. N. *Oncogene* **2003**, *22*, 9075–9086.

- (51) Short, N. J.; Kantarjian, H.; Ravandi, F.; Daver, N. *Ther. Adv. Hematol.* **2019**, *10*, 204062071982731.
- (52) Jia, J.; Zhu, F.; Ma, X.; Cao, Z.; Cao, Z. W.; Li, Y.; Li, Y. X.; Chen, Y. Z. *Nat. Rev. Drug Discov.* **2009**, *8*, 111–128.
- (53) Antolin, A. A.; Workman, P.; Mestres, J.; Al-Lazikani, B. *Curr. Pharm. Des.* **2017**, *22*, 6935–6945.
- (54) Li, C.; Liu, L.; Liang, L.; Xia, Z.; Li, Z.; Wang, X.; McGee, L. R.; Newhall, K.; Sinclair, A.; Kamb, A.; Wickramasinghe, D.; Dai, K. *Mol. Cancer Ther.* **2015**, *14*, 375–83.
- (55) Hart, S.; Goh, K. C.; Novotny-Diermayr, V.; Tan, Y. C.; Madan, B.; Amalini, C.; Ong, L. C.; Kheng, B.; Cheong, A.; Zhou, J.; Chng, W. J.; Wood, J. M. *Blood Cancer J.* **2011**, *1*, No. e44.
- (56) Tanabe, K. *Int. J. Mol. Sci.* **2017**, *18*, 2508.
- (57) Silva, A. M. S.; Tavares, H. R.; Barros, A. I. N. R. A.; Cavaleiro, J. A. S. *Spectrosc. Lett.* **1997**, *30*, 1655–1667.
- (58) Boumendjel, A.; Boccard, J.; Carrupt, P. A.; Nicolle, E.; Blanc, M.; Geze, A.; Choisnard, L.; Wouessidjewe, D.; Matera, E. L.; Dumontet, C. *J. Med. Chem.* **2008**, *51*, 2307–2310.
- (59) Christensen, L. P.; Lam, J.; Thomasen, T. *Phytochemistry* **1990**, *29*, 3155–3156.
- (60) Manzoor, S.; Bilal, A.; Khan, S.; Ullah, R.; Iftikhar, S.; Emwas, A. H.; Alazmi, M.; Gao, X.; Jawaid, A.; Saleem, R. S. Z.; Faisal, A. *Sci. Rep.* **2018**, *8*, 3305.